Journal of Physical Sciences, Vol. 13, 2009, 261-273
ISSN: 0972-8791 : www.vidyasagar.ac.in/journal

Quasi Resonant Tunneling Lifetime in Multibarrier System Under the Action of Electricfield

S. P. Bhattacharya

Department of Physics & Technophysics
Vidyasagar University
Midnapore-721102, West Bengal

Received November 4, 2009; accepted November 18, 2009

ABSTRACT

In the unbiased periodic MBS the resonant tunneling corresponds to unit transmission coefficient across the structure. With the application of low and moderate dc-electric fields, the tunneling energy spectrum (quasiresonant) of the MBS gets Stark shifted and the transmittance for some of the resonance-type peaks gets lowered compared to those in the field-free case due to gradual localization of wave functions which can be explained using bending band picture. In this context for a biased MBS, the carrier lifetime under quasiresonant condition can be termed as quasiresonant tunneling lifetime (QRTL). The QRTL is the most important parameter that has to be determined for realizing the tunable quantum cascade laser [3-5] on the basis of Wannier-Stark ladder (WSL). The theoretical investigations of lifetime has been reported for the double-barrier systems (DBSs) [6-11], MBSs [12-13], and SLs [14-17] in the absence of external dc-electric field and also for the dc-biased quantum wells [18-19], DBSs [20], and SLs [21]. But none of them has addressed the response of QRTL to the applied field for individual quasiresonant states in an electrically biased MBS, which would be the key issue in modeling high-speed RT devices. We address these aspects in the following sections.

2. Introduction

The widely mentioned features such as transmission coefficient, resonant tunneling energy levels, current density, and negative differential conductivity which provide signatures of resonant tunneling in device applications of semiconductor MBSs are enlightened in earlier works. These fundamental properties of tunneling have built up a profound understanding in the researchers through continuous and effective studies. Although exhaustive studies on the resonant tunneling lifetime in case of periodic MBSs have been performed both experimentally and theoretically, the research on tunneling lifetime in aperiodic systems is recently gaining momentum. The discovery of quasicrystal has accelerated the study of quasiperiodic MBSs arranged according to the standard generalized Thue-Morse and generalized

Fibonacci sequences. Ideal aperiodic SLs show a highly fragmented and fractal-like electronic spectrum with self-similar patterns with the presence of localized, extended and critical states [28-30]. A lot of theoretical works regarding the band structures, transmission properties, density of states, localization of wave functions, trace map and Landauer resistances etc. in the unbiased and electrically biased quasiperiodic MBSs are already discussed by several authors. But very little attention [31] has been paid for the study of electric-field-induced tunneling lifetime (QRTL) in the quasiperiodic systems like the generalized Fibonacci multibarrier systems (GFSs) and the generalized Thue-Morse multibarrier systems (GTSs). Earlier authors have shown that the tunneling states in a miniband of the electrically biased periodic MBS exhibit some anomalous behavior in carrier lifetime [24]. This level-wise study of lifetime and the corresponding behavior have motivated us to study these aspects related to field-dependent tunneling lifetime in quasiperiodic MBSs. Regarding quasiperiodic systems, it is worth mentioning that the generalized Fibonacci sequence is in frequent use to study the transport properties; but the use of the generalized Thue-Morse sequence is quite limited both in theory and experiment.

In view of the above discussion, a detailed analysis of QRTL has been presented in case of quasiperiodic MBSs (e.g., GFS and GTS) in the presence of external dc fields. For the calculation of QRTL across multibarrier systems, our computational model based on the transfer-matrix formalism using exact Airy function approach and a search technique is same as discussed by Nanda etal.. Moreover, the average escape rate across the different structures mentioned above has also been numerically computed and discussed.

3. Models for different quasiperiodic multibarrier systems:

In the present theoretical model, both the periodic and the generalized quasiperiodic multibarrier structures have been grown along the *z*-axis starting from the two basic building blocks A and B [32]. Here the block A (B) consists of a rectangular quantum well of thickness '*a*' and a rectangular barrier of thickness '*b*' ('b'').

Table-1. A few initial generations of generalized Fibonacci sequence for different values of *n* and *m* with initial conditions, S_{-1} = B and S_0 = A

t	S_t	$S_t = [1[S_{t-1}].1[S_{t-2}]]$	S_t	$S_t = [2[S_{t-1}].1[S_{t-2}]]$	S_t	$S_t = [1[S_{t-1}].3[S_{t-2}]]$
1	S_1	AB	S_1	AAB	S_1	ABBB
2	S_2	ABA	S_2	AABAABA	S_2	ABBBAAA
3	S_3	ABAAB				
4	S_4	ABAABABA				
5	S_5	ABAABABAABAAB				

Table-2. A few initial generations of generalized Thue-Morse sequence for different values of *n* and *m* with initial condition, S_0= {A,B}

T	S_t	$S_t = \left[1[S_{t-1}].1[\bar{S}_{t-1}]\right]$	S_t	$S_t = \left[2[S_{t-1}].2[\bar{S}_{t-1}]\right]$	S_t	$S_t = \left[1[S_{t-1}].3[\bar{S}_{t-1}]\right]$
1	S_1	ABBA	S_1	ABABBABA	S_1	ABBABABA
2	S_2	ABBABAAB				
3	S_3	ABBABAABBAABABBA				

The present block model of periodic MBS has been generated by iterating A and B alternatively, so that the t^{th} generation of the system is given by, $S_t = t[AB]$, where t stands for the number of repetitions.

4. Theoretical framework

The QRTL, τ, is calculated on the basis of the energy uncertainty relation [6] given as:

$$\tau = \frac{\hbar}{2\Delta\varepsilon_m} \tag{1}$$

where $\Delta\varepsilon_m$ is the half-width at half-maximum of the quasiresonant transmission peak corresponding to RT at energy ε_m. The main advantages of this method are that it is straightforward and it provides same degree of accuracy compared with other different methods [7,9,22-23]. So the derivation of QRTL requires the knowledge of quasiresonant transmission spectrum. For the purpose, a GaAs-$Al_xGa_{1-x}As$ MBS have been considered under a uniform electric field (E) applied along the growth direction (z). The transmission coefficient (T_c) for this system has been obtained through the theoretical model based on the transfer matrix approach using exact Airy function formalism and effective mass dependent boundary conditions:

$$T_c = \left|\frac{\det[T_N]}{(T_N)_{22}}\right|^2 \tag{2}$$

Here, $[T_N]$ refers the transfer matrix that relates the coefficient matrices of the incoming and outgoing waves in the N-barrier system.

The transmission spectrum is obtained on the basis of Eq. (2) for a range of incident energies of electrons at different values of the dc field. From the transmission spectrum for a particular value of the field, the energy (ε_m) corresponding to each quasiresonant transmission peak and the energies on both sides of the peak corresponding to T_c at half the transmission maxima are obtained using a search technique [13]. Then one can find the half-width at half-maxima ($\Delta\varepsilon_m$) corresponding to the quasiresonant energy, ε_m from the difference of the two energies corresponding to half maxima. Finally, $\Delta\varepsilon_m$, thus obtained, is used to compute the QRTL, τ, using Eq. (1).

5. Numerical Analysis

The carrier lifetimes are computed for the 5-unit cell GaAs - 5-unit cell $Al_{0.3}Ga_{0.7}As$ MBS for the below-barrier states ($0 < \varepsilon \le V_0$, V_0 being conduction band discontinuity) with the number of barriers, N = 2, 3, 4 and 6 both in unbiased and dc-biased situations with varying electric field. It is worth mentioning that for $\varepsilon \le V_0$ only one allowed miniband with (N-1) number of resonant states occurs in each of the field-free N-barrier system. For this GaAs-$Al_{0.3}Ga_{0.7}As$ system, the numerical parameters (e.g., V_0, electron effective masses, the lattice constants) are same as in section 4.1C of the previous chapter. Here also, we have considered both the well and barrier widths each consisting of 5 unit cells and the field intensity of 1 V/m as the field-free case.

Now we think it is worthwhile to present the algorithm (stepwise) of the search program used for locating the maxima, minima, and the half-widths of the resonant transmission peaks and to compute the resonant tunneling lifetime.

Step 1: The transmission coefficient (T_c) for a N-barrier system is computed for incident energies, ε, in the range 0-0.3701 eV [$0 < \varepsilon \le V_0$] with a step length of 0.00001 eV, on the basis of Eq. (5.1.2). The results are stored in a data file as n, $\varepsilon(n)$ [= $0.00001 * n$ eV] and $T_c(n)$.

Step 2: $T_c(1)$ = 0 and is taken as the minimum to the left of the first transmission maximum. Hence we set $n_{\min l}$ = 1, $\varepsilon_{\min l}$ = $\varepsilon(1)$, and $(T_c)_{\min l}$ = $T_c(1)$, respectively.

Step 3: The maximum is searched by an iterative process starting from $n = n_{\min l}$ onwards and satisfying the condition $T_c(n-m) \le T_c(n) \ge T_c(n+m)$ for m = 1, 2, .., 9 and $T_c(n-10) \prec T_c(n) \succ T_c(n+10)$. The corresponding values are stored as $n_{\max} = n$, $\varepsilon_{\max} = \varepsilon(n)$, and $(T_c)_{\max} = T_c(n)$, respectively.

Step 4: The left half-maximum of the peak is defined as $(T_c)_{\mathrm{m}idl}$ = $[(T_c)_{\min l} + (T_c)_{\max}]/2$. Now by iteration starting from $n = n_{\min l}$ to $n_{\max}$, the corresponding value of energy at half-maximum is found for which $\left|(T_c)_{\mathrm{m}idl} - (T_c)_n\right|$ is the smallest. Then these data are saved as $n_{\mathrm{m}idl} = n$, $\varepsilon_{\mathrm{m}idl} = \varepsilon(n)$, and $(T_c)_{\mathrm{m}idl} = T_c(n)$, respectively.

Step 5: The minimum of the peak on the right-side of maximum is found by an iterative process starting from $n = n_{\max}$ onwards and satisfying the condition $T_c(n-m) \ge T_c(n) \le T_c(n+m)$ for m = 1, 2, .., 9 and $T_c(n-10) \succ T_c(n) \prec T_c(n+10)$. The respective values are stored as $n_{\min r} = n$, $\varepsilon_{\min r} = \varepsilon(n)$, and $(T_c)_{\min r} = T_c(n)$, respectively.

Step 6: The right half-maximum of the peak is defined as $(T_c)_{\mathrm{m}idr} = [(T_c)_{\max} + (T_c)_{\min r}]/2$. The corresponding value of energy at half-maximum is found for which $\left|(T_c)_{\mathrm{m}idr} - (T_c)_n\right|$ is the smallest by the iteration technique starting from $n = n_{\max}$ to $n_{\min r}$. The corresponding values are stored as $n_{\mathrm{m}idr} = n$, $\varepsilon_{\mathrm{m}idr} = \varepsilon(n)$, and $(T_c)_{\mathrm{m}idr} = T_c(n)$, respectively.

Step 7: The width at half-maximum of the resonant peak is equal to the difference, $(\varepsilon_{\mathrm{m}idr} - \varepsilon_{midl})$. Then the resonant lifetime for the corresponding resonant energy $\varepsilon_{\max}\ (\varepsilon_m)$ is computed on the basis of Eq. (1).

Step 8: The right minimum of the previous peak is the left minimum for the succeeding peak. Hence we reset $n_{\min l} = n_{\min r}$, $\varepsilon_{\min l} = \varepsilon_{\min r}$, and $(T_c)_{\min l} = (T_c)_{\min r}$ and Step 3 to Step 8 are repeated until all the data points are exhausted.

6. Results and discussion

In this section we have discussed the results obtained on the tunneling lifetime corresponding to the resonant tunneling states for both field-free and biased MBSs. The field-free case is presented to better comprehend the effect of electrical bias on the QRTL in biased systems. The variation of RTL with resonant energy (ε_m) corresponding to the tunneling miniband in field-free condition for the 5-unit cell GaAs - 5-unit cell $Al_{0.3}Ga_{0.7}As$ periodic MBS with N = 3, 4, and 6 is presented in Fig.1. In case of the triple-barrier system having two resonant states, it is prominent that the resonant state with higher ε_m has lower lifetime as a consequence of higher group velocity. Looking at the curves corresponding to N = 4, and 6, we observe that the QRTL is minimum at the center of the miniband for unbiased MBSs. It suggests that an electron with ε_m in the middle of the miniband would tunnel out faster than the ones with values of ε_m near the band edge. The result is analogous to those for semiconductor MBSs with rectangular potential barriers dealt with the field-free infinite Kronig-Penney model, where the group velocity becomes maximum near the middle of the allowed miniband [12-13].

In Fig. .2(a and b), we have plotted the tunneling coefficient vs incident energy which give us the resonant tunneling energies, in fig 2 (c and d)we have plotted the variation of QRTL for each tunneling state lying in the miniband for the periodic MBSs with varying number of barriers with respect to the applied electric field in the range 1V/m to 10 MV/m for a periodic MBS and a fibonacci type MBS respectively. The curves of Fig.2(c and d) depict that the QRTL remains almost constant (shown by break) for fields up to 100 kV/m. In this field the states get Stark shifted but the shift being in the order of 10^{-4} eV, is very small compared to the miniband level-separation. So the wave functions corresponding to these states remain extended in nature and the coupling between wells suffers no significant

change. As a result, the resonant tunneling velocity remains almost same up to this field.

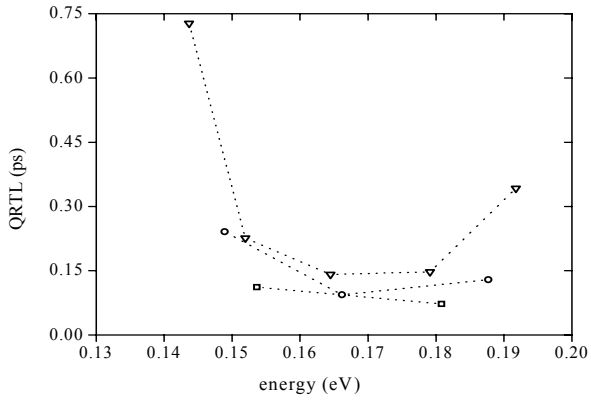

Fig.1: Variation of RTL with incident energy (ε) in case of the 5-unit cell GaAs - 5-unit cell $Al_{0.3}Ga_{0.7}As$ MBS in field-free condition. Square, circle, and inverted triangle symbols correspond to the number of barriers (N) = 3, 4, and 6, respectively. The data points for a particular set are joined by dotted lines for better visual convenience.

In Fig.2(a), the tunneling coefficient shows that with increase in field the tunneling coefficient decreases. QRTL in DBS is found to decrease almost linearly with increasing electric field beyond 100 kV/m. In case of two quasiresonant states in triple-barrier system, and that the carrier corresponding to higher ε_m has lower lifetime for low fields as in case of unbiased condition. At higher fields, the QRTL for the higher state increases with field whereas reverse is the case for the lower state. It is also worthwhile to note that there exists a particular electric field, E_c (~ 4.4 MV/m) where both the higher and lower states have the equal value of tunneling lifetime, τ_c (0.076 ps). In the triple-barrier system the electron in each state tunnels with the same group velocity when the applied electric field becomes equal to E_c. Here, E_c and τ_c are referred to as the characteristic field and the characteristic lifetime, respectively, for the miniband of an N-barrier MBS [24].

In Figs2(c)-(d) the variation of QRTL with respect to the applied electric field has been shown for $N > 3$ for a periodic and aperiodic system respectively. The variation of QRTL for quasiresonant tunneling energies in the miniband under biased condition ($E \leq 500$ kV/m) is similar with the field-free case where the electrons having energies near the middle of the miniband have larger group velocity and thus the minimum lifetime in comparison to those of the band-edge states.

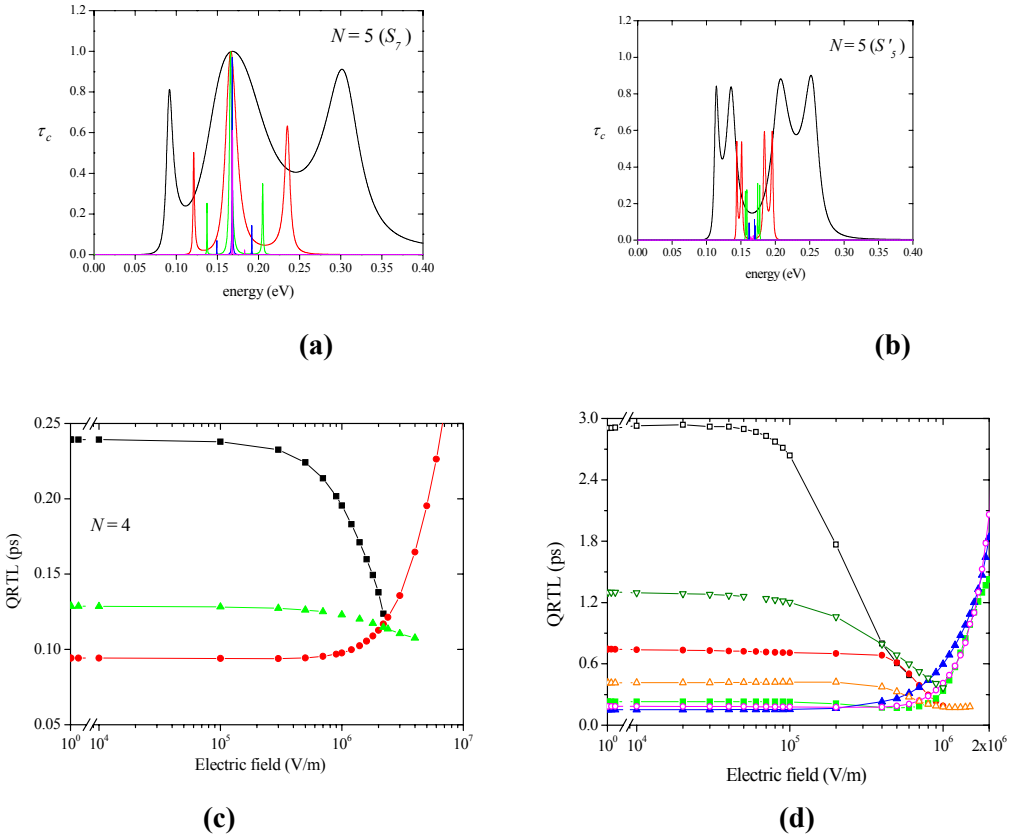

Fig.2(a,b). Variation of transmission coefficient (T_c) versus incident electron energy (ε) (0–0.4 eV) for number of barrier cells, n_b = 1 (Black), 2 (Red), 3 (Green), 4 (Blue), 5 (Magenta) in case of total number of barriers, N = 5 for (a) the first kind (S_7), and (b) the second kind (S'_5) GFS using the GaAs-$Al_{0.3}Ga_{0.7}As$ system in unbiased condition(.C) and (D)Plot of QRTL versus applied dc electric field in 5-unit cell GaAs - 5-unit cell $Al_{0.3}Ga_{0.7}As$ periodic MBS for different number of barriers (N) and for Fibonacci lattice of first kind respectively. L1 (Black solid square); L2 (Red open circle); L3 (Green open triangle); L4 (Blue open square); L5 (Magenta solid inverted triangle)

For fields larger than 500 kV/m, the curves depict a contrasting behavior between the lifetime for quasiresonant states located at the band edge and those located well inside the miniband. With the increase in electric field, the QRTL corresponding to the mid-band state increases whereas it decreases for the states lying near the miniband edges. The decrease in QRTL for the states at lower band edge is sharp but a slow rate of decrement in QRTL is found for the upper band-edge states. In each of the cases, it is found that the QRTL corresponding to all the energy states in the miniband becomes almost equal (τ_c) at the field, E_c. The

values of E_c corresponding to this miniband for N = 4 and 6 are 2.3 and 1.34 MV/m, respectively. The respective τ_c values are: 0.12 and 0.19 ps. It is clearly observed that E_c shifts towards the lower value but τ_c becomes larger with the increase in number of barriers. In this context it is worthwhile to mention that the states near the centre of the miniband starts forming partial WSL for fields which satisfy the relation [Eq. (3.2.1)], $eEd > (\Delta\varepsilon)/2$, $\Delta\varepsilon$ being the maximum level-separation in the absence of field [25]. More and more states join the partial WSL as the inequality becomes more and more pronounced and the band forms a complete WSL for fields which satisfy the inequality [Eq. (3.2.2)], $eEd > \varepsilon_{bw}$, where ε_{bw} is the width of the miniband. For N = 4 and 6, the maximum level-separations, $\Delta\varepsilon$, in the miniband are 0.0215 and 0.0146 eV, respectively. As a result, the minimum field strengths (E) required for the formation of partial WSL near the centre of the miniband in case of N = 4 and 6 are calculated as 1.90 and 1.29 MV/m, respectively. Here, it is observed that the characteristic field (E_c) for a particular MBS is slightly higher than the minimum field (E) which satisfies the existence condition for partial WSL in that MBS. The increase in QRTL for the mid-band states which are expected to form WSL states is a natural consequence of localization. The band-edge states which have not joined the WSL follow the general pattern of increase in group velocity with the increase in field and hence causing a decrease in QRTL.

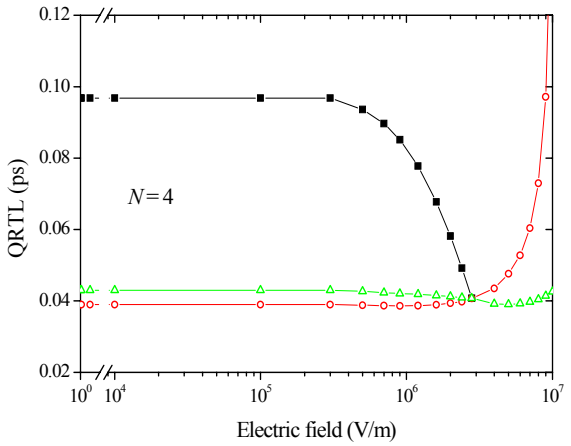

Fig.3. Plot of QRTL versus applied dc electric field in the 7-unit cell GaAs - 3-unit cell $Al_{0.3}Ga_{0.7}As$ MBS for N = 4. L1 (Black solid square,); L2 (Red open circle); L3 (Green open triangle); where L1-L3 correspond to the quasiresonant energy states (e.g., '1' for minimum energy state) in the miniband.

To examine the broader range of validity of the results regarding E_c and τ_c in MBSs we consider systems with the variation in barrier width, well width and number of barriers. It is found that for N = 3 and 4 the features presented in Figs..2(b)-(c) remain valid as long as the sum of the unit cells in well (n_w) and

barrier (n_b) materials is maintained at a minimum of 10 unit cells in a period subjected to the condition $n_b > 2$. As an example, in Fig.3 the variation of QRTL versus field is presented for $N = 4$ of a 7-unit cell GaAs - 3-unit cell $Al_{0.3}Ga_{0.7}As$ system. Further, for $N = 6$ the features of Fig2(d) are reproducible when the minimum number of unit cells in a period (n_b plus n_w) remains at 8 with $n_b > 2$.

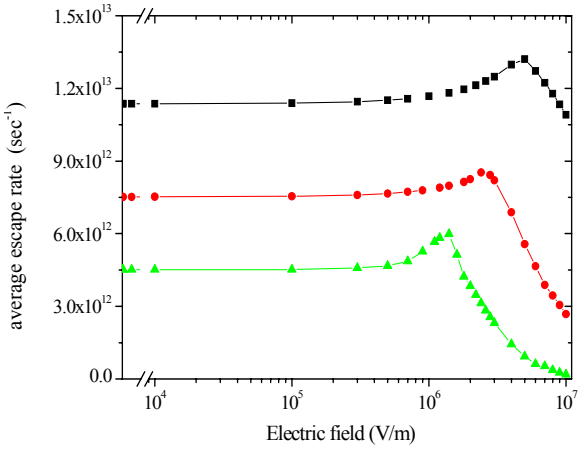

Fig4. Plot of average escape rate versus applied dc electric field in the 5-unit cell GaAs - 5-unit cell $Al_{0.3}Ga_{0.7}As$ MBS for different number of barriers, $N = 3$ (Black), 4 (Red), 6 (Green).

From the above discussion it is clear that the lifetime of different quasilevels in the miniband is different at any given electric field, except for E_c. Again the inverse of QRTL for a quasilevel gives the escape rate [26]. By averaging $1/\tau$ values over all the states in a miniband, the average escape rate has been obtained, which has a direct bearing on the tunneling current, the most important aspect in resonant tunneling through the MBS. Here, the average escape rate is computed for 5-unit cell GaAs - 5-unit cell $Al_{0.3}Ga_{0.7}As$ MBSs with $N = 3$, 4 and 6 and the corresponding variation with the applied electric field is shown in Fig. 5.1.4. The curves show that average escape rate always assumes lower values for higher N at a given field and this feature is a consequence of tunneling through a longer system. The average escape rate remains almost constant up to the field ~ 100 kV/m, then exhibits a small resonance-type peak and finally decreases at high field. The resonance-type peak occurs at the characteristic field (E_c) and results in the maximum escape rate. The same qualitative feature has also been reported by Wacker et al [27]. The above discussions lead us to the fact that E_c and τ_c can be considered as the characteristic parameters of a particular MBS. So the quantum transport through the MBS could be controlled by selecting the proper characteristic field tailored by the choice of suitable parameters in the MBS.

7. Conclusion

Based on the method involving half-width at half-maximum the lifetime of the quasiresonant states of MBS have been studied in the presence of uniform electric field. Two characteristic parameters are addressed relating to the electric-field induced resonant transport phenomena. The existence of the characteristic field which represents the synchronization of carrier velocity associated with all the quasiresonant states and corresponds to the maxima in the average escape rate, is an interesting outcome of the present theoretical investigation in ballistic transport of carriers through an MBS. The characteristic field corresponds to a field strength which favors the existence of partial WSL in the miniband. Especially, the characteristic parameters E_c and τ_c coming from the numerical simulation might have an application for high-speed electronic and optoelectronic devices e.g., one can construct a velocity selector with the proper choice of n_b, n_w and N related to the MBS so that it tunnels out mono-velocity carriers with the maximum escape rate at that characteristic field E_c.

The present block model of periodic MBS has been generated by iterating A and B alternatively. we have chosen the blocks A and B both containing a layer of the well material of width 'a' in combination with a layer of the barrier material of different widths 'b' and 'b'', respectively. In such a situation, the barrier width between two consecutive wells will have variable width where the widths of barrier layers will be multiples of a definite width.

The t^{th} generation of any kind of the generalized Fibonacci sequence [33] has been framed using the following recursion rule: $S_t = \left[n[S_{t-1}].m[S_{t-2}] \right]$, for $t > 0$. Here n and m give the number of repetitions of the associated generation. A given pair of values (n,m) represents a particular kind of the generalized Fibonacci sequence, e.g., (n=1, m=1), (n=2, m=1) and (n=1, m=3) are taken as the first, the second, and the third kinds, respectively. The initial conditions for the generation of any kind of this type of sequence are chosen as S_{-1} = B and S_0 = A.

The different generations of the generalized Thue-Morse sequence [34] have been coined using the iteration formula: $S_t = \left[n[S_{t-1}].m[\overline{S}_{t-1}] \right]$, for $t > 0$. $\overline{S}_{t-1}$ is the complement of S_{t-1} obtained by interchanging A and B. In this case the pair of values (1,1), (2,2) and (1,3) for (n,m) are referred to as the first, the second, and the third kinds of the generalized Thue-Morse sequence, respectively. Here the initial condition is chosen as S_0 = {A,B} for all kinds.

In the present work the comparative analysis of QRTL among the different quasiperiodic multibarrier systems has been performed with the incident electron energies in below-barrier condition ($\varepsilon \le V_0$, V_0 being the barrier height). The basic system is considered as GaAs-$Al_{0.3}Ga_{0.7}As$ MBS. Block A consists of a GaAs layer of 5-unit cell thick followed by $Al_{0.3}Ga_{0.7}As$ layer of 5-unit cell thick while block B consists of a 5-unit cell thick GaAs layer followed by a 5-unit cell thick $Al_{0.3}Ga_{0.7}As$ layer. It may be mentioned that in below-barrier condition, only one allowed energy

miniband exists for all the systems under investigation. Here each of the aperiodic systems has been studied taking all the three kinds with a constant number of barriers. The applied homogeneous electric field across the structure has been varied from 1 V/m to 2 MV/m. Here also the electric field of strength 1V/m is treated as the unbiased condition.

8. Results and discussion

It is worth pointing here that in a typical periodic MBS there exists a characteristic electric field where all the states have equal value of tunneling lifetime i.e., electrons associated with these states tunnel out with the same group velocity at that characteristic field [24]. But in all the cases of quasiperiodic systems such complete synchronization in carrier velocities for all the states has not been achieved, yet some sort of partial synchronization [37] in lifetime (in other words, carrier velocity) occurs for most of the quasiresonant states [within the field-regime (~ 700-900 kV/m) i.e., the lifetimes for most of the states come sufficiently close in magnitude at that field regime. This finding has a resemblance with the resonance-type peaks in the variation of average escape rate with the applied field for all the systems considered. As the tunneling current has direct dependence on average escape rate, it is worthwhile to explore the impact of applied electric field on average escape rate in the quasiperiodic systems like periodic cases. The average escape rate has been obtained by averaging the reciprocals of QRTL values over all the states in a miniband for each of the three kinds of mentioned GFS and GTS (N = 8 for each) under biased condition and the corresponding variation with field is presented. The case of block periodic MBS is also shown for the effective comparison with the quasiperiodic cases. The average escape rate remains almost constant up to the field ~ 100 kV/m, then exhibits a small resonance-type peak resulting in the maximum escape rate and finally decreases at high field. We observe that the resonance-type peaks for all the systems occur for a particular field-domain (~ 700-900 kV/m) where a partial synchronization-like behavior of tunneling lifetimes for the quasiresonant levels is observed. So it can be inferred that a certain field-domain tunes all the systems to give the maximum escape rates according to their structures.

The average escape rate for the block periodic case appears to be less in comparison with that for each quasiperiodic system. The rate of increase of average escape rate (near the maximum) with the applied field has been found to depend on the degree of quasiperiodicity. But an interesting observation is that for the second and third kinds, the peaks in average escape rate for the GFSs are less sharp than those for the GTSs whereas the peak in case of the GFS is sharper compared to that in the GTS concerning the first kind. Since the sharp variation of average escape rate near its maximum can be exploited for device applications, we can therefore conclude that the first kind of GFS and the second and third kinds of GTS are most favorable for the design of resonant tunneling devices. As the higher kinds of aperiodic systems are more aperiodic in nature, the above findings show that the periodicity of the GFS and the quasiperiodicity of the GTSL promise wider scopes for device applications.

An attempt has been made to explore the impact of quasiperiodicity on the resonant tunneling lifetime in electrically biased semiconductor multibarrier systems. We have addressed various important issues regarding quasiperiodicity to explore the new directions of analyzing high-speed semiconductor devices. The use of block periodic and aperiodic MBSs is one of the aspects of present motivation. The incorporation of quasiperiodicity modifies the internal potential of the system in the presence of external dc fields and originates extra regions of positive differential lifetime for some of the quasiresonant energy levels. In case of the generalized Fibonacci and Thue-Morse MBSs the degree of quasiperiodicity affects in reverse order for the middle and near band-edge states of the miniband. An interesting outcome of the present investigation is that the observation of a synchronization-like behavior (to some extent) of tunneling lifetimes for the qusiresonant levels in all the quasiperiodic systems in the field-domain (~700-900 kV/m) has a close resemblance with the resonance-type peaks in the variation of average escape rate with the applied field for all the systems considered. In the context of analyzing the ultrahigh-speed electronic devices the presence of sharp resonance-type peaks in average escape rate might play a crucial role. The sharpness of resonance-type peaks favors the control of average escape rate (around the peak) through the systems by the slight change in field. So the applied electric field can act as a probe to opt the required rate of escape for quasiperiodic systems having sharp peaks. To conclude, it can be emphasized that the lower kind of GFS and the higher kind of GTS are most suitable for resonant tunneling device applications.

REFERENCES

1. E. H. Hauge and J. A. Støvneng, Rev. Mod. Phys. 61, 917 (1989)
2. R. Landauer and Th. Martin, Rev. Mod. Phys. 66, 217 (1994)
3. C. Sirtori, P. Kruck, S. Barbieri, P. Collot, J. Nagle, M. Beck, J. Faist, and U Oesterle, Appl. Phys. Lett. 73, 3486 (1998)
4. Y. Ergün, M. Hoştut, S. U. Eker, and İ. Sökman, Superlatt. Microstruc. 37, 163 (2005)
5. P. K. Mahapatra, S. Sinha, and P. Panchadhyayee, Physica B 403, 3365 (2008)
6. P. J. Price, Phys. Rev. B 38, 1994 (1988)
7. C. J. Arsenault and M. Meunier, Phys. Rev. B 39, 8739 (1989)
8. A. M. Elabsy, Physica B 292, 233 (2000)
9. H. Z. Xu and M. Okada, Physica B 305, 113 (2001)
10. O. A. Tretiakov, T. Gramespacher, and K. A. Matveev, Phys. Rev. B 67, 073303 (2003)
11. H. Wang, H. Xu, and Y. Zhang, Phys. Lett. A 355, 481 (2006)
12. A. Khan, P. K. Mahapatra, and C. L. Roy, Phys. Lett. A 249, 512 (1998)
13. J. Nanda, P. K. Mahapatra, and C. L. Roy, Physica B 383, 232 (2006)
14. J.-W. Choe, H.-J. Hwang, A. G. U. Perera, S. G. Matsik, and M. H. Francombe, J. Appl. Phys. 79, 7510 (1996)
15. P. Pereyra, Phys. Rev. Lett. 84, 1772 (2000)
16. A. Khan, P. K. Mahapatra, S. P. Bhattacharya, and S. N. Mohammad, Phil. Mag. 84, 547 (2004)

17. C. Pacher, W. Boxleitner, and E. Gornik, Phys. Rev. B 71, 125317 (2005)
18. G. G. de la Cruz, I. Delgadillo, and A. Calderón, Solid State Comm. 98, 357 (1996)
19. K. R. Lefebvre and A. F. M. Anwar, IEEE J. Quantum Electron. 33, 187 (1997)
20. N. Zou, J. Rammer, and K. A. Chao, Phys. Rev. B 46, 15912 (1992)
21. B. Rosam, K. Leo, M. Glück, F. Keck, H. J. Korsch, F. Zimmer, and K. Köhler, Phys. Rev. B 68, 125301 (2003)
22. A. F. M. Anwar, A. N. Khondker, and M. R. Khan, J. Appl. Phys. 65, 2761 (1989)
23. E. Anemogiannis, E. N. Glytsis, and T. K. Gaylord, IEEE J. Quantum Electron. 29, 2731 (1993)
24. P. Panchadhyayee, R. Biswas, A. Khan, and P. K. Mahapatra, J. Appl. Phys. 104, 084517 (2008)
25. P. K. Mahapatra, K. Bhattacharyya, A. Khan, and C. L. Roy, Phys. Rev. B 58, 1560 (1998)
26. M. Tsuchiya, T. Matsusue, and H. Sakaki, Phys. Rev. Lett. 59, 2356 (1987)
27. A. Wacker, A-P Jauho, S. Rott, A. Markus, P. Binder, and G. H. Döhler, Phys. Rev. Lett. 83, 836 (1999)
28. E. Maciá, Rep. Prog. Phys. 69, 397 (2006)
29. E. Maciá and F. Domínguez-Adame, Phys. Rev. Lett. 76, 2957 (1996)
30. R. P.-Álvarez, F. G.-Moliner, and V. R. Velasco, J. Phys. Condens. Matt. 13, 3689 (2001)
31. E. Reyes-Gómez, C. A. Perdomo-Leiva, L. E. Oliveira, and M. de Dios-Leyva, J. Phys. Condens. Matt. 10, 3557 (1998)
32. F. Laruelle, B. Etienne, J. Barrau, K. Khirouni, J. C. Brabant, T. Amand, and M. Brousseau, Surf. Sci. 228, 92 (1990)
33. G. Gumbs and M. K. Ali, Phys. Rev. Lett. 60, 1081 (1988)
34. M. Kolar, M.K. Ali, and F. Nori, Phys. Rev. B43, 1034 (1991)
35. M. H. Tyc and W. Salejda, Physica A 303, 493 (2002)
36. P. Panchadhyayee, R. Biswas, A. Khan, and P. K. Mahapatra, J. Phys. Condens. Matt. 20, 275243 (2008)
37. P. Panchadhyayee, R. Biswas, C. Sinha, and P. K. Mahapatra, J. Phys. Condens. Matt. 20, 445229 (2008)